Nonlinear Finite Element Analysis of Prestressed Concrete Tee Beams

Dr. Ihsan A.S. Al-Shaarbaf * & Dr. May J. Hamoodi **

Received on: 11/5/2008
Accepted on: 7/8/2008

Abstract

A three-dimensional finite element computer program (3DMPCP) has been developed to investigate the behaviour of prestressed reinforced concrete beams and to predict their ultimate loads. To verify the ability of this computer program in predicting the correct behaviour of prestressed concrete beams, analysis of a simply supported prestressed reinforced concrete tee beam was carried out. The beam section is 1.12 m deep, 2.44 m flange width and it is designed for a span of 32.3 m from support to support. The test load, 0.85(1.4 DL. + 1.7 LL.), was applied to the beam and flexural cracks were observed at midspan. The finite element analysis has indicated that numerical load-central deflection curve obtained is in good agreement with the experimental one. The analysis also gives the expectation for the ultimate load value. Distribution of concrete normal stress throughout a cross section and along the beam, at different stages of loading , are presented .

Keywords: Finite element, Nonlinear analysis, Prestressed beams, T-beams.

التحليل اللاخطي باستخدام طريقة العناصر المحددة للعتبات المسبقة الجهد وذات المقطع T

الخلاصه

في هذه الدراسه تم تطوير برتامج الحاسوب (3DMPCP) المتخصص باستخدام طريقه العناصر المحدده للتحليل اللاخطي للاعضاء الخرسانيه المسلحه المسبقه الجهد. ولبرهنه قدره هذا البرنامج على التوقع الصحيح لتصرف هذه الاعضاء اثناء التحميل , فقد تم استخدام البرنامج في تحليل عتبه خرسانيه مسبقه الجهد معرضه للانحناء. ان هذه العتبه كانت بطول 32،3م و بمقطع على شكل حرف T له عمق كلي مقداره 1،12م وعرض شفه بمقدار 2،44م. ان الحمل المسلط على العتبه كان بمقدار 85 ٪ من مجموع الاحمال المعامله الميته و الحيه . ولقد لوحظ ظهور التشققات الناتجه عن الانحناء في وسط العتبه ,عند بلوغ نهايه التحميل.
التحليل الذي اجري للعتبه باستخدام طريقه العناصر المحدده أظهران منحني الاحمال-الانحراف الوسطي للعتبه الذي تم الحصول عليه ,هو في توافق جيد مع ذلك الذي تم الحصول عليه من الفحص المختبري. كذلك فان التحليل يعطى توقع لقيمه الحمل الاقصى للعتبه.
وفي هذا البحث عرض توزيع الاجهادات الخرسانيه على كامل عمق المقطع العرضي للعتبه وكذلك على الامتداد الطولي لها ,وعند مختلف مراحل التحميل.

* Civil Engineering Department, Collage of Engineering, Al-Nahrain University /Baghdad
** Building and Construction Engineering Department, University of Technology /Baghdad

Introduction

The presence of compressive stresses in the concrete due to prestressing helps the beams in resisting the applied moment effectively and leads to reduce deflections under service conditions. Through the computer program 3DMPCP, the behaviour of a prestressed beam is simulated up to the ultimate failure load .The effect of the pre-tensioning is considered as well as a reduction in the yield stress of the tendons. Elasto-plastic work hardening model is used to represent concrete in compression , while concrete in tension is simulated by a fixed smeared crack model .Quadratic hexahedral brick elements are used to model the concrete. Reinforcing bars are modeled as axial members embedded within the brick elements, and perfect bond between concrete and bars is assumed to occur [1].

Finite Element Formulation

The application of the finite element method falls into equilibrium problems. A body may be subjected to a force acting through its volume ,

$$\{P\}=[P_x\ P_y\ P_z]^T \qquad ....(1)$$

The Cartesian coordinate system is used to describe the directions of the components of the force. Any particle in the body may undergo a displacement having components u, v and w in x , y and z-directions respectively ,

$$\{d\}=[u\ \ v\ \ w]^T \qquad .....(2)$$

The relations between the strain components and the displacement components have terms of first order partial derivatives,

$$\{e\}=\begin{bmatrix} e_x \\ e_y \\ e_z \\ g_{xy} \\ g_{yz} \\ g_{zx} \end{bmatrix}=\begin{bmatrix} \frac{\partial}{\partial x} & 0 & 0 \\ 0 & \frac{\partial}{\partial y} & 0 \\ 0 & 0 & \frac{\partial}{\partial z} \\ \frac{\partial}{\partial y} & \frac{\partial}{\partial x} & 0 \\ 0 & \frac{\partial}{\partial z} & \frac{\partial}{\partial y} \\ \frac{\partial}{\partial z} & 0 & \frac{\partial}{\partial x} \end{bmatrix}\begin{bmatrix} u \\ v \\ w \end{bmatrix} ..(3a)$$

$$\{e\}=[A][d] \qquad .....(3b)$$

and the corresponding vector of stress is given by,

$$\{s\}=[s_x\ \ s_y\ \ s_z\ \ t_{xy}\ \ t_{yz}\ \ t_{zx}]^T \ .(4)$$

The two vectors of stress and strain are related through the constitutive matrix as,

$$\{s\}=[D]\ \{e\} \qquad .....(5)$$

Isoparametric brick elements of 20 nodes have been used to represent the concrete continuum , Fig.1. The displacement vector at any point within the element, and the nodes displacements vector,[a], are related as,

$$\{d\}^e=[\mathrm{N}]\{\mathrm{a}\}^e \qquad .....(6)$$

where [N] is a matrix containing the Serendipity shape functions. The substitution of Eq.[6] into [5] gives a relation between the strains and the nodal displacements of the element,

$$\{e\}^e = [B]\{a\}^e \qquad .....(7)$$

Matrix [B] gives values of strain at any point within the element, due to unit values of nodal displacements.

As [D] matrix is defined to take into account the material nonlinearities , the stiffness matrix of the assemblage can be written as,

$$[K] = \sum_n \int_{v^e} [B]^T [D][B] dv^e \qquad .....(8)$$

Modeling of concrete material

Concrete has a complex behaviour involving phenomena such as cracking and inelastic response. Its behaviour in compression differs from that in tension, as it is well known. Therefore the [D] matrix must consist of two parts.

The behaviour of *concrete in compression* is simulated by an elasto-plastic work hardening model followed by a perfectly plastic plateau, which is terminated at the onset of crushing , Fig.2.The non-linear deformations occur when it is stressed beyond the limit,

$$\sigma_o = c_p f_c' \qquad .....(9)$$

where , c_p is the plasticity coefficient and has a value of 0.3 to represent the behaviour of normal concrete. In the inelastic range the equivalent stress is given by,

$$s_e = c_p f_c' + E\left[e_c - \frac{c_p f_c'}{E}\right] - \frac{E}{2e_o'}\left[e_c - \frac{c_p f_c'}{E}\right]^2 \qquad .....(10)$$

Where e_o' is defined in Fig.2.

The *yield criterion* depends on two stress invariants($I_1$and J_2) and it can be expressed as,

$$f(\{s\}) = c\, I_1 + \left[(c\, I_1)^2 + 3\, b\, J_2\right]^{\frac{1}{2}} = s_o \quad ..(11)$$

The material parameters c and b are equal to 0.17734 and 1.35468, respectively[1]. I_1 is the first stress invariant and, J_2 is the second deviatoric stress invariant.

As the concrete is stressed beyond its initial yielding surface, in the three-dimensional stress space shown in Fig.3, an isotropic hardening rule is assumed to describe the growth of subsequent loading surfaces. At this stage the total concrete strain, e_c , can be decomposed into elastic and plastic components as,

$$e_c = e_e + e_p \qquad .....(12)$$

and the stress becomes the effective stress, $\bar{s}$, which can be expressed as a function of the plastic strain as,

$$\bar{s} = c_p f_c' - E\, e_p + \left(2\, E^2\, e_o'\, e_p\right)^{\frac{1}{2}} \quad ..(13)$$

The slope of the effective stress-plastic strain curve is the hardening coefficient (H'),

$$H' = \frac{d\bar{s}}{de_p} = E\left[\left[\frac{e_o'}{2e_p}\right]^{\frac{1}{2}} - 1.0\right] \quad ...(14)$$

In order to establish the stress-strain relation in the plastic range , the plastic strain increment vector , $\{de^p\}$, is assumed to be proportional to a vector normal to the current loading surface known as the *flow vector* , $\partial f(\{s\})/\partial\{s\}$,

$$\{de^{p}\} = dl\,\frac{\partial f(\{s\})}{\partial\{s\}} \qquad \text{....(15)}$$

The relationship in Eq.[15] is known as the *flow rule* . dl is a proportionality factor has a positive value and can be found as:

$$dl = \left[\frac{\{a\}^{T}[D]}{H' + \{a\}^{T}[D]\{a\}}\right] d\{e\} \qquad \text{....(16)}$$

where [D] is the elastic constitutive matrix, and $\{a\}$ represents the flow vector.

The total incremental strain vector is the sum of elastic and plastic components. It can be written with the use of Eqs.[12], [15] and [16] as:

$$\{de\} = [D]^{-1} d\{s\} + \left[\frac{\{a\}^{T}[D]}{H'\{a\}^{T}[D]\{a\}}\right] d\{e\}\{a\} \qquad \text{.(17)}$$

By multiplying both sides of Eq.[17] by the [D] matrix , the complete elasto-plastic incremental stress-strain relationship may be obtained as:

$$d\{s\} = [D]^{ep}\, d\{e\} \qquad \text{.....(18)}$$

where $[D]^{ep}$ is the elasto-plastic stiffness matrix which can be written as,

$$[D]^{ep} = \left[[D] - \frac{[D]\{a\}\{a\}^{T}[D]}{H' + \{a\}^{T}[D]\{a\}}\right] \qquad \text{.(19)}$$

As crushing stage is reached in concrete, its stresses drop to zero and it is assumed to lose its resistance completely against any further deformation. Therefore, the crushing failure may be controlled simply by a surface in the strain space . *Crushing criterion* can be obtained by converting the yield criterion given in Eq.[11] into strains ,

$$c\,I_1' + \left[(c\,I_1')^2 + 3\,b\,J_2'\right]^{\frac{1}{2}} = e_{cu} \qquad \text{..(20)}$$

where , I_1' is the first strain invariant, J_2' is the second deviatoric strain invariant and e_{cu} is the ultimate strain.

Behaviour of *concrete in tension* is mainly controlled by a cracking phenomenon[2]. The smeared crack approach has been employed in the finite element analysis. In this approach the cracked concrete is assumed to remain a continuum, and the local discontinuities due to cracking are distributed over the volume of the sampling point under consideration. According to this cracking model, a crack is assumed to occur in a plane normal to the direction of the maximum principal tensile stress. The limiting tensile stress required to define the onset of cracking , s_{cr}, can be calculated as follows:

a)for the triaxial tension zone,

$$s_{cr} = f_t \qquad \text{...(21)}$$

b)for the tension-tension-compression zone,

$$s_{cr} = f_t\left[1 + \frac{0.75\,s_3}{f_c'}\right] \qquad \text{....(22)}$$

c) for the tension-compression-compression zone,

$$s_{cr} = f_t\left[1 + \frac{0.75 s_2}{f_c'}\right]\left[1 + \frac{0.75 s_3}{f_c'}\right] \qquad \text{..(23)}$$

where , s_1 , s_2 and s_3 are the principal stresses, f_t and f_c' are the tensile and compressive concrete strengths respectively, and are both given positive values.

As the cracking criterion is violated, the concrete behaviour becomes orthotropic with the direction of orthotropy coinciding with the direction of major principal stress (s_1), since the plane of failure is assumed to be perpendicular to this direction. The normal and shear stresses across the failure plane are reduced as well as their stiffness. However, the concrete between two adjacent failure planes remains capable of sustaining tensile stresses. Thus the cracked [D] matrix for the incremental stress-strain relationship in the local material axes (1,2,3) may be written as :

$$[D_{cr}]_L = \begin{bmatrix} E_1 & 0 & 0 & 0 & 0 & 0 \\ 0 & \frac{E}{(1-n^2)} & \frac{nE}{(1-n^2)} & 0 & 0 & 0 \\ 0 & \frac{nE}{(1-n^2)} & \frac{E}{(1-n^2)} & 0 & 0 & 0 \\ 0 & 0 & 0 & b_1 G & 0 & 0 \\ 0 & 0 & 0 & 0 & G & 0 \\ 0 & 0 & 0 & 0 & 0 & b_1 G \end{bmatrix} \quad \text{....(24)}$$

where , E_1 is the reduced modulus of elasticity in the planes perpendicular to the cracked plane, $b_1 G$ is the reduced shear modulus in the cracked plane and n is Poisson's ratio. Because of the lack of interaction between the orthogonal planes due to the cracking, Poisson's ratio is set to zero. The matrix given in Eq.[24] can be expressed in the global coordinate axes as,

$$[D_{cr}]_G = [T]^T [D_{cr}]_L [T] \quad \text{....(25)}$$

where $[T]$ is the coordinate transformation matrix.

To improve the realism of the post-cracking behaviour of concrete , the *tension-stiffening* effect is considered.The bilinear model shown in Fig.4, has been used to represent the gradual release of tensile stresses normal to the cracked plane as the crack width increases.Also the cracked reinforced concrete retains shear stiffness due to the aggregate interlock at the crack interfaces and the dowel action of reinforcing bars crossing the crack. So, a reduction in shear modulus is considered by using a shear reduction factor, b . The value of this factor ranges between zero and one as in *shear retention* model given in Fig.5.

Modeling of Steel Reinforcement

The embedded representation is used to model the steel reinforcement. The reinforcing bar is considered to be an axial member built into the isoparametric concrete element, Fig.1, and a perfect bond between the steel and the concrete is assumed to occur. The stress-strain behaviour of steel can be assumed to be identical in tension and compression. The uni-axial behaviour of reinforcement is simulated by an elastic-linear work hardening model.

The prestressing tendons are tensioned between external end anchorages to an *initial prestress* of about 70% of the characteristic strength[3].The initial stresses at transfer, become reduced because of the losses in tension caused by slip in the grips, elastic compression, and friction[4]. Thus, the yield stress considered for the tendons in the

finite element analysis carried out through the developed computer program, is given as:

$$\left(f_{py}\right)_{adj} = f_{py} - f_{ts} \qquad \text{....(26)}$$

where, $\left(f_{py}\right)_{adj}$ is the adjusted yield stress and f_{ts} is the tensile stress in the tendons after the losses.

Prestressing Representation in the Computer Program

The aim of the developed computer program 3DMPCP is to consider the effect of the pre-tensioning or the post-tensioning tendons on the hardened concrete. During the transferred of the forces to the concrete by bond stress, the concrete will be pre-compressed before applying the service load. In the computer program , compressive forces are applied at the ends of the member within few increments. The value of a compressive force is equal to initial stressing force of the tendon minus the expected losses, and it is applied to the concrete at nodes representing the position of prestressing tendons. After that the external service loads will be applied to the member .The computer program also considers the camber effect in calculating the central deflection of a prestressed member.

Nonlinear Solution Techniques

The combined incremental-iterative technique is used to conduct the nonlinear finite element analysis .The total external load is subdivided into smaller increments, and within each increment of loading , iterative cycles are performed in order to obtain a converging solution . The modified Newton-Raphson method is used to solve the governing equations . According to this method the stiffness matrix is not necessarily to be updated for each iteration. The stiffness matrix, through this computer program , is updated at 2 nd., 7 th, 12 th, iterations of each increment of loading.The convergencec haracteristics of this method can be improved by the inclusion of *line searches* acceleration technique.The progress of the iterative procedure is monitored with a force convergence criterion. The percentage of the norm of out of balance force vector to the norm of external applied load vector should not be greater than 2%.

Application

The precast prestressed concrete single tee beam was planned for the roof structure of a public bus garage[5]. Following the manufacture of 40 percent of these roof beams, it was found that the compressive concrete strength of 28-day cylinder was slightly below the specified value ($f_c^{'}$ = 41.4 MPa). The lower concrete strength prompted the owner to question the suitability and structural adequacy of the single tee beams.

The single prestressed tee beam, which has been analysed , was approximately 33.7m long designed to a span 32.3m with 1.4m cantilever overhang, Fig.6 . The flange and web steel reinforcement consisted of welded wire fabric with prestressing strands located in the web,Fig 7. The strands were of Grade 270, 13 mm diameter, and low-relaxation. Each strand has seven wires and it was initially stressed to approximately 135.7 kN. The beam was manufactured from sand-lightweight concrete.

The test of the beam was conducted in accordance with chapter 20 of the

ACI Building Code[6]. Test load was equivalent to 0.85(1.4D+1.7L).Precast concrete panels, weighing 28 kN each, were used for loading the beam uniformly.

The finite element *analysis* of the prestressed concrete beam has been carried out by using the developed computer program 3DMPCP. By taking advantage of symmetry , a segment representing one quarter of the beam was used in the analysis. The segment considered was modeled by using 40 elements of quadratic hexahedral brick element type, Fig.8.

The *results* obtained from the analysis are given below :

1- The numerical load-deflection curve and the experimental one are shown in Fig.9. The figure reveals that good agreement has been obtained between the experimental and the finite element results throughout the entire range of the test load .

2- The numerical ultimate load-deflection curve and the experimental load-deflection curve are shown in Fig.10. In this figure, the expected ultimate load for the prestressed beam is 26.7% greater than the test load which is equivalent to about 0.85(1.4D + 1.7L).

3- The distribution of concrete normal stress along the depth of the cross-section of the beam is shown in Fig.11.The cross-section is located at a distance of 1.3 m from midspan of the beam. The figure indicates that the compressive stress due to prestressing has a higher value at the bottom of the web and lower value at top of the flange. As the beam is loaded, there is a continuous decrease in the compressive stresses below the neutral axis and a continuous increase at the top part of the section. At 70% of the test load, the extreme bottom of the web becomes in tension. At 85% of the test load, different behaviour is noticed because of the appearance of flexural crack. At 100% of the test load there is a sudden decrease in tensile stress at the bottom of the section and a noticed increase in compressive stress at the top flange. Also a shift in the position of neutral axis, towards the top face, is noticed because of the growth of crack.

4- The distribution of the normal concrete stress along half of the span is shown in Fig.12. The stresses are measured at sampling points located at a distance of 203mm from the bottom face of the web. The figure shows that the higher prestressing normal stresses are within the middle third of the span and the lower values are at regions close to the supports. As the beam is loaded, the compressive stresses within the middle third, increased towards zero value and then to tensile stresses. Lower increase in normal stresses can be noticed close to the ends.

Conclusions

1- It is verified that the computer program [3DMPCP] is able to predict the behaviour of prestressed concrete beams.

2- Accurate results in the analysis has been obtained by using the adjusted value of the yield stress of the tendons.

3- The prestressing normal stress, at concrete sampling points within a section of the beam, has different values. The higher compressive stresses are at the area of tendons position.

4- It is found that the ultimate load of the prestressed beam is about 26% higher than the designed test load. Therefore, the developed computer program can be considered as a good tool in the non-destructive tests.

Notations

[A] displacement gradient matrix
{a} nodal displacements, or flow vector
[B] strain - nodal displacement matrix
c_p plasticity coefficient
[D] constitutive matrix
$[D]^{ep}$ elasto-plastic constitutive matrix
$[D_{cr}]$ cracked constitutive matrix
$d\,l$ plastic multiplier
E modulus of elasticity
$f_c^{'}$ uniaxial compressive strength of concrete
f_t uniaxial tensile strength of concrete
f_{py} yield stress of tendon
f_{ts} tensile stress in the tendon after the losses
G shear modulus
$H^{'}$ hardening parameter
I_1 first stress invariant
$I_1^{'}$ first strain invariant
J_2 second deviatoric stress invariant
$J_2^{'}$ second devistoric strain invariant
[K] stiffness matrix
[N] shape functions
{P} body forces
[T] transformation matrix
u, v, w displacement components
$\{e\}$ strain vector
e_{cu} ultimate strain of concrete
e_p plastic strain
$e_o^{'}$ total strain corresponding to the parabolic part of uniaxial compressive stress-strain curve of concrete
n Poisson's ratio
$\{s\}$ stress vector
s_o equivalent stress
$\bar{s}$ effective stress
s_1, s_2, s_3 principal stresses
s_{cr} cracking stress
$\{d\}$ displacement vector

References

[1]-Al- Shaarbaf, I.A.S., "Three-Dimensional Nonlinear Finite Element Analysis of Reinforced Concrete Beams in Torsion", Ph. D. Thesis, University of Bradford, U.K., 1990, 323 pp.

[2]-Chen, W. F., "Plasticity in Reinforced Concrete", McGraw – Hill Book Company, New York, 1982, 474 pp.

[3]-Kong,F.K., and Evans, R.H., " Reinforced and Prestressed Concrete",2 nd Edition, Nelson,U.K., 1980,412 pp.

[4]-Ramaswamy,G.S.,"Modern Prestressed Concrete Design", Pitman, U.K., 1978,175pp.

[5]-Anderson, N.S., and Popovic, P.L.,"Load Testing of Long Span Prestressed Single Tee Beams", PCI Journal , Vol.33 No.2 , March / April 1988, pp42-51.

[6]-ACI Committee 318,"Building Code Requirements for Reinforced Concrete (ACI 318-83)", Concrete Institute, Detroit, Michigan.

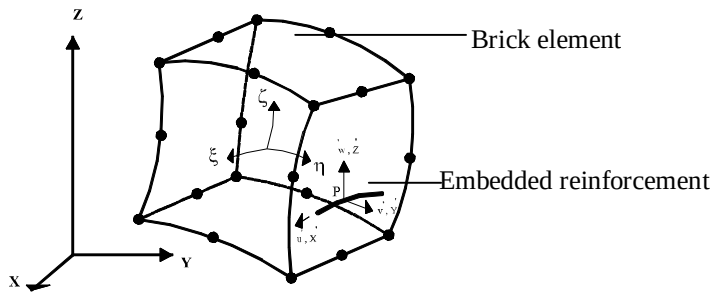

Figure (1) Twenty-node isoparametric brick element with embedded representation of reinforcement.

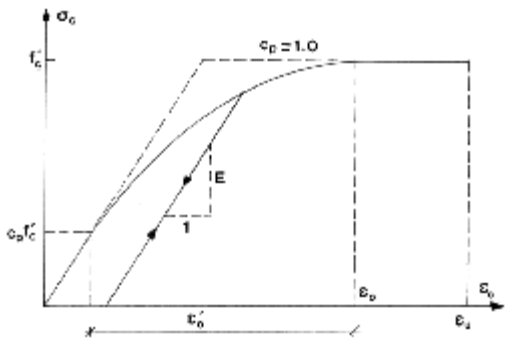

Figure(2) Uniaxail stress-strain curve for concrete in compression.

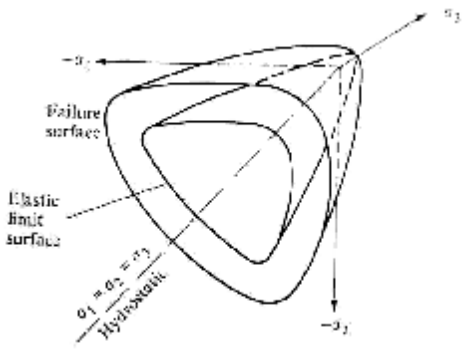

Figure(3) Failure surface of concrete in three-dimensional stress space.

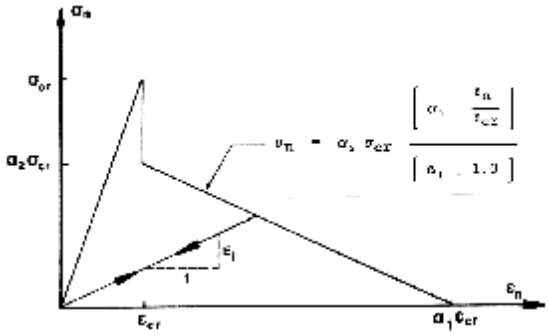

Figure (4) Tension-stiffening model for cracked concrete.

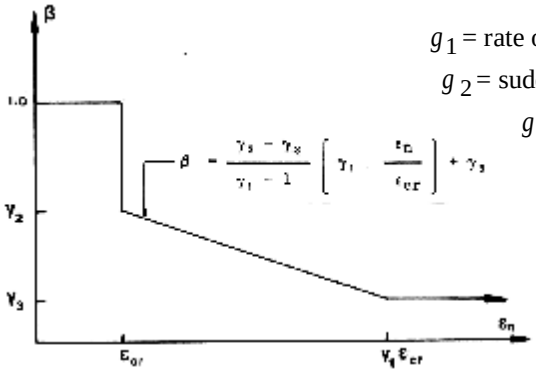

g_1 = rate of decay of shear stiffness.
g_2 = sudden loss in shear stiffness.
g_3 = residual shear stiffness.

Figure (5) Shear retention model for cracked concrete

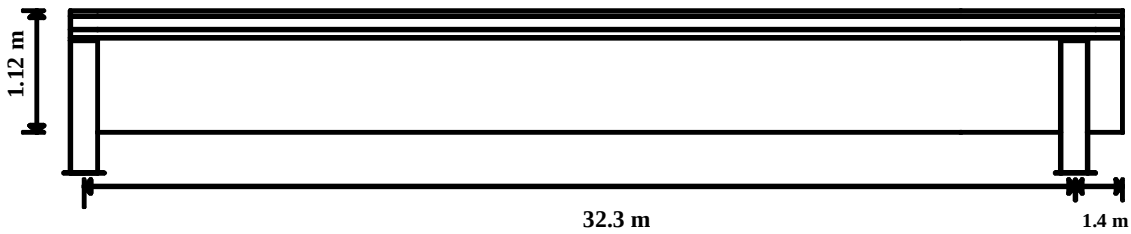

Figure (6) Elevation of the selected prestressed concrete tee beam.

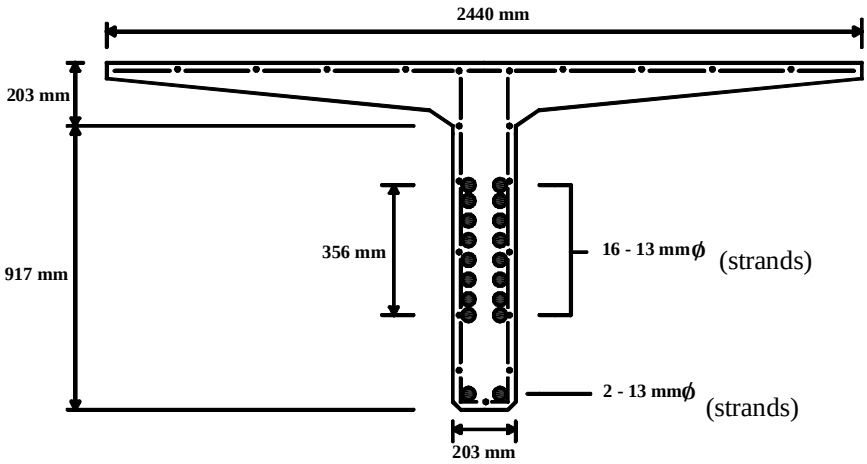

Figure (7) Cross section of the selected prestressed concrete tee beam.

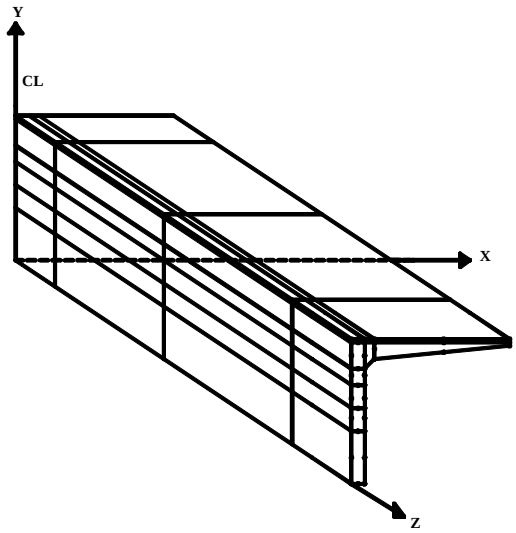

Figure (8) Finite element mesh used in the analysis (one quarter).

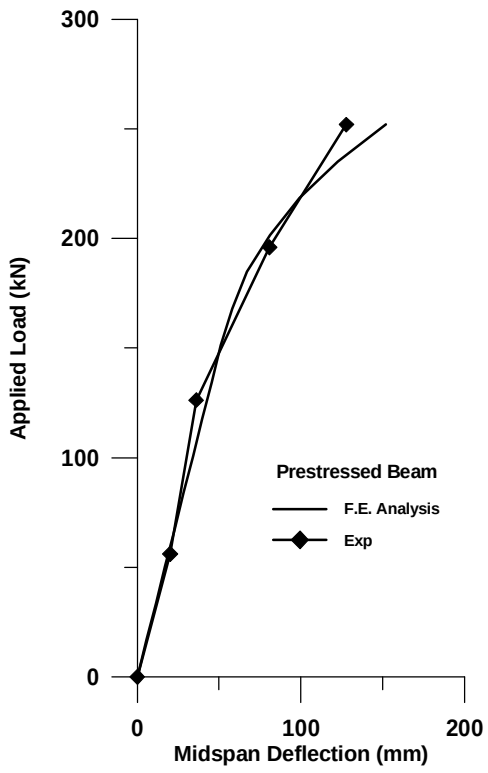

Figure (9) Experimental and numerical load-deflection behavior up to the test load.

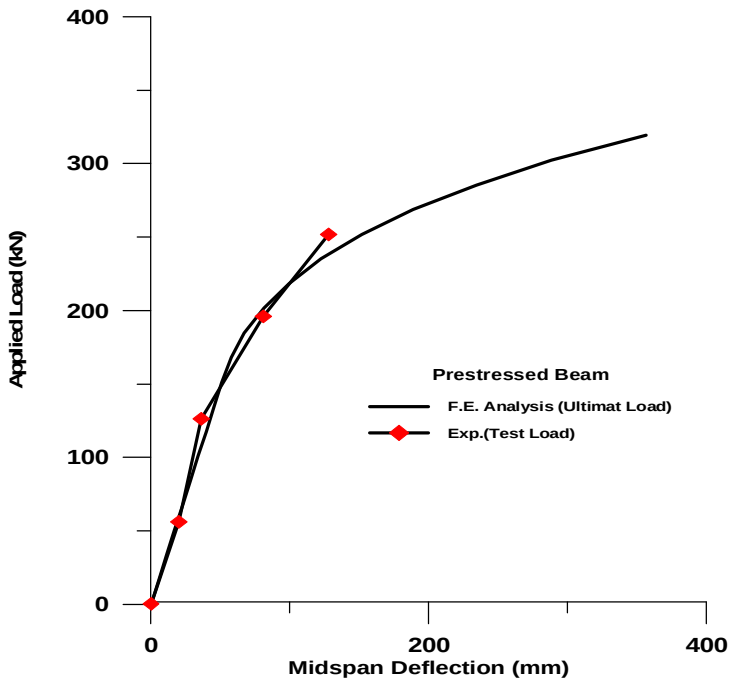

Figure (10) Numerical load-deflection behavior up to the ultimate load.

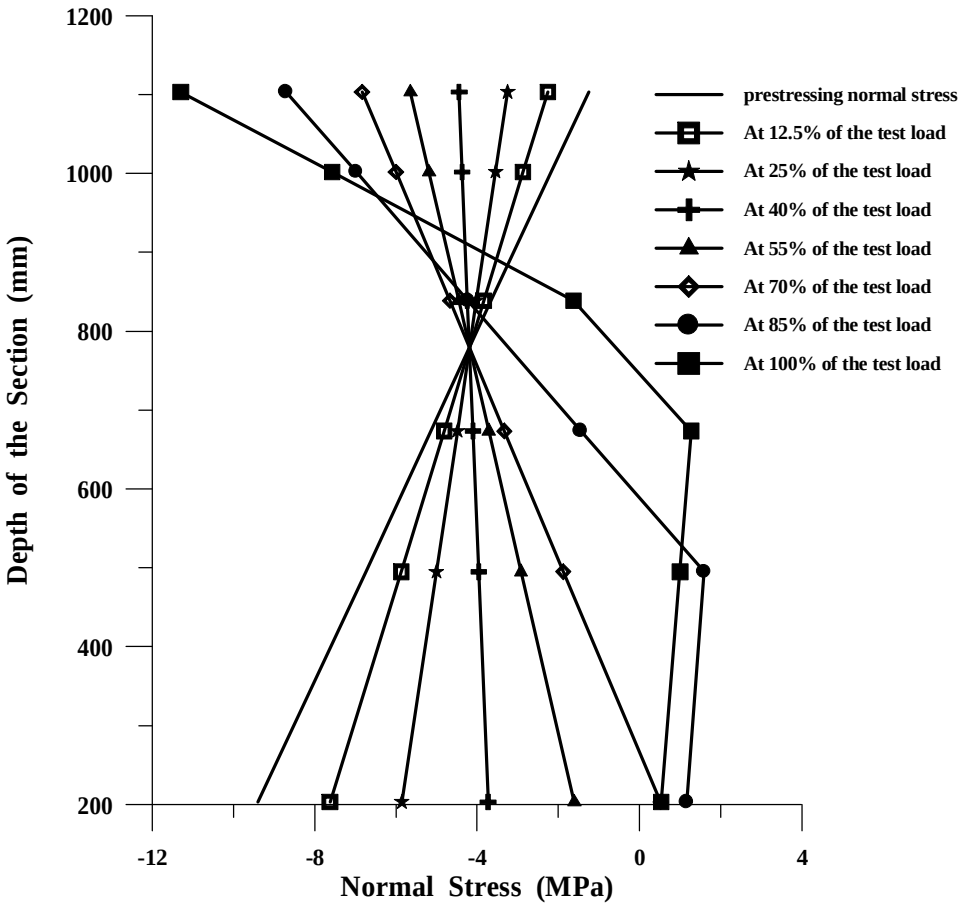

Figure (11) Distribution of concrete normal stress at a distance of 1.3m from midspan. at different stages of loading.

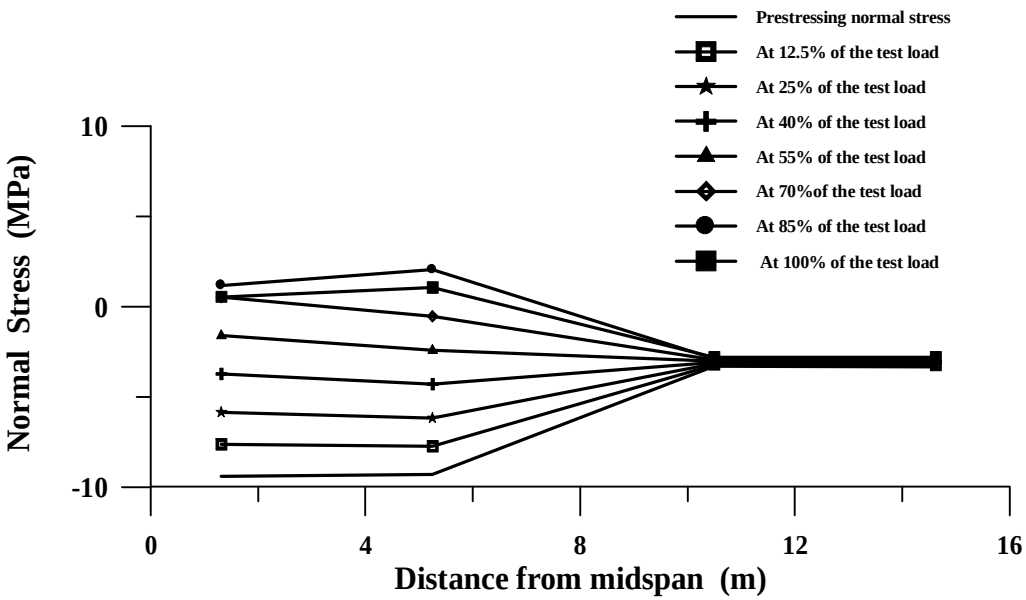

Figure (12) Distribution of concrete normal stress along half of the span. at different stages of loading.